Published online 13 January 2017

Nucleic Acids Research, 2017, Vol. 45, No. 8 ***4743–4755***
doi: 10.1093/nar/gkw1332

Differential hepatitis C virus RNA target site selection and host factor activities of naturally occurring miR-122 3′ variants

Daisuke Yamane[1,2,*], Sara R. Selitsky[1,3,4], Tetsuro Shimakami[1,5], You Li[1,2], Mi Zhou[1,3,4], Masao Honda[5], Praveen Sethupathy[1,3,4] and Stanley M. Lemon[1,2,*]

[1]Lineberger Comprehensive Cancer Center, The University of North Carolina at Chapel Hill, Chapel Hill, NC 27599, USA, [2]Departments of Medicine and Microbiology & Immunology, The University of North Carolina at Chapel Hill, Chapel Hill, NC 27599-7292, USA, [3]Bioinformatics and Computational Biology Curriculum, The University of North Carolina at Chapel Hill, Chapel Hill, NC 27599, USA, [4]Department of Genetics, The University of North Carolina at Chapel Hill, Chapel Hill, NC 27599, USA and [5]Department of Gastroenterology, Kanazawa University Graduate School of Medicine, Kanazawa, Ishikawa 920-8641, Japan

Received April 19, 2016; Revised December 10, 2016; Editorial Decision December 19, 2016; Accepted December 22, 2016

ABSTRACT

In addition to suppressing cellular gene expression, certain miRNAs potently facilitate replication of specific positive-strand RNA viruses. miR-122, a proviral hepatitis C virus (HCV) host factor, binds and recruits Ago2 to tandem sites (S1 and S2) near the 5′ end of the HCV genome, stabilizing it and promoting its synthesis. HCV target site selection follows canonical miRNA rules, but how non-templated 3′ miR-122 modifications impact this unconventional miRNA action is unknown. High-throughput sequencing revealed that a 22 nt miRNA with 3′G ('22–3′G') comprised <63% of total miR-122 in human liver, whereas other variants (23–3′A, 23–3′U, 21–3′U) represented 11–17%. All loaded equivalently into Ago2, and when tested individually functioned comparably in suppressing gene expression. In contrast, 23–3′A and 23–3′U were more active than 22–3′G in stabilizing HCV RNA and promoting its replication, whereas 21–3′U was almost completely inactive. This lack of 21–3′U HCV host factor activity correlated with reduced recruitment of Ago2 to the HCV S1 site. Additional experiments demonstrated strong preference for guanosine at nt 22 of miR-122. Our findings reveal the importance of non-templated 3′ miR-122 modifications to its HCV host factor activity, and identify unexpected differences in miRNA requirements for host gene suppression versus RNA virus replication.

INTRODUCTION

Persistent infection with hepatitis C virus (HCV) is a leading cause of chronic liver diseases, including cirrhosis and liver cancer (1,2). A member of the *Flaviviridae* family, HCV possesses a positive-sense RNA genome that contains a large single open reading frame (ORF) that encodes three structural and seven non-structural proteins that contribute collectively to viral RNA synthesis and the subsequent assembly and egress of new virions (3). The ORF is flanked by 5′ and 3′ untranslated RNA (UTR) segments that contain regulatory elements that are important for translation and replication (4). Infection with HCV is highly hepatotropic, and dependent upon the host factor activity of microRNA-122 (miR-122), a liver specific microRNA (miRNA) that accounts for a large fraction of all miRNAs in the liver (5–7). miR-122 binds two tandem sites, designated S1 and S2, near the 5′ end of the HCV RNA genome as a complex with Argonaute 2 (Ago2) protein, a key component of the miRNA-induced RNA silencing complex (miRISC) (7–10). This results in protection of the viral RNA from 5′ decay mediated by the cytoplasmic 5′ exoribonuclease, Xrn1 (8,11–12) and independently stimulates *de novo* viral RNA synthesis directed by the viral NS5B RNA-dependent RNA polymerase (13). Collectively, these actions are essential for efficient production of infectious virus (7), a fact borne out by the substantial antiviral activity of miR-122 antagomirs administered to HCV-infected individuals (14).

*To whom correspondence should be addressed. Tel: +1 919 843 1848; Fax: +1 919 843 7240; Email: yamane@email.unc.edu
Correspondence may also be addressed to Stanley M. Lemon. Tel: +1 919 843 1848; Fax: +1 919 843 7240; Email: smlemon@med.unc.edu
Present address: Daisuke Yamane, Department of Microbiology and Cell Biology, Tokyo Metropolitan Institute of Medical Science, Kamikitazawa, Setagaya-ku, Tokyo, 156-8506, Japan.

While unusual, this positive host factor activity of miR-122 in a viral lifecycle is not unique among miRNAs. miR-17 and let-7 family members have recently been found to positively regulate the replication of pestiviruses, veterinary pathogens with positive-strand RNA genomes distantly related to HCV (15). These miRNAs primarily target sites in the 3′UTR of these viruses rather than the 5′UTR. The binding of miR-17 to bovine viral diarrhea virus RNA results in small positive effects on its stability, but is critically important for replication (15). At a mechanistic level, it is not clear that miR-17 and let-7 function in a manner similar to miR-122 in the HCV lifecycle, but these recent observations show that the capacity to positively regulate positive-strand virus replication is common to multiple miRNAs. Whether rules governing miRNA target selection in this context are similar to those acting in miRNA suppression of host gene expression is unknown, and an interesting question.

miR-122 binds to sites throughout the HCV RNA genome with relatively low affinity (16), but it is the robust binding of miR-122 to the S1 and S2 sites in concert with Ago2 that accounts for its pro-viral HCV host factor activity (7–8,10). The structural basis for this robust binding is not well understood. Mutational studies have demonstrated the importance of canonical seed sequence base pairing, as well as 3′ supplemental interactions, in the binding of miR-122 to HCV RNA and in the recruitment of Ago2 to both the S1 and S2 sites (17–19) (Figure 1A). Studies using selective 2′-hydroxyl acylation analyzed by primer extension (SHAPE) have also provided insight into the interactions of miR-122 with the HCV target sequence *in vitro* (20,21), but these are biased by the absence of Ago2. Other host RNA-binding proteins, such as poly(C)-binding protein 2 (PCBP2), are also likely to influence miR-122 interactions with the HCV genome (22). Thus, despite its importance in the viral lifecycle, the structure of the complex formed by the viral RNA, miR-122 and Ago2 remains unknown.

Existing models for this complex include no base-pair interactions between HCV RNA and the 3′ terminal nucleotides of the miRNA (Figure 1A), but no previous studies have carefully examined the role of the 3′ miR-122 sequence in HCV target site selection. Recent studies indicate that the 3′ ends of guide-strand RNAs may regulate guide-target pairing affinities by influencing the conformation of both the Argonaute protein and guide strand RNA through their interaction with the PAZ domain (23–25). In addition, CLEAR-CLIP studies have suggested that duplex formation between the RNA target and the 3′ end of miRNAs contributes significantly to target site selection for many miRNAs (26). Since the 3′ terminal nucleotides of miR-122 (and other miRNAs) undergo extensive non-templated additions and deletions *in vivo* (27), we sought to understand whether variation at the 3′ end of miR-122 influences its HCV host factor activity. Here, we describe the diversity of 3′ miR-122 sequences that are present within infected and uninfected human liver tissue, as well as the role played by the 3′ terminal nucleotides of miR-122 in S1 and S2 target site selection, and in recruiting Ago2 to the HCV genome and stabilizing and promoting its replication. Our results demonstrate that both length and composition of the 3′ terminal nucleotides strongly influence the HCV host factor activity of naturally occurring miR-122 variants, but have surprisingly little if any effect on canonical miR-122 function in suppressing gene expression. We also show that there are novel and distinct requirements for miR-122 binding and Ago2 recruitment at the S1 versus S2 sites of the HCV genome.

MATERIALS AND METHODS

Ethics statement

All human subjects provided written informed consent for participation in the study, and tissue acquisition procedures were approved by the ethics committee for Human Genome/Gene Analysis Research at Kanazawa University (Kanazawa, Japan).

Small RNA-sequencing

RNA was isolated as described previously (28). RNA purity was assessed with a Nanodrop 2000 (Thermo Scientific) and integrity was determined with an Agilent 2100 Bioanalyzer (Agilent). RNA integrity and sequencing quality were comparable for all specimens. Small RNA libraries were generated using Illumina TruSeq Small RNA Sample Preparation Kit (Illumina, San Diego, CA, USA). Sequencing was performed on an Illumina HiSeq 2000 platform. For the bioinformatics analysis, miR-122-5p variants differing in their 3′ terminal sequence were identified by searching for all small RNA reads in each sample that shared the core 5′ miR-122 sequence (nts 1–18): 'UGGAGUGUGACAAUGGUG'. These reads were categorized according to their downstream 3′ sequence as described in 'Results' section and shown in Figure 1B, and the proportion of all miR-122 reads represented by each specific variant determined for each tissue or cell culture sample. Nineteen variants accounted for >98% of all miR-122 reads in each of the samples (Figure 1B), and include the most common variants described by Katoh *et al.* (27): 21–3′U (UGGAGUGUGACAAUGGUGUUU), 22–3′G (UGGAGUGUGACAAUGGUGUUUG), 23–3′U (UGGAGUGUGACAAUGGUGUUUGU) and 23–3′A (UGGAGUGUGACAAUGGUGUUUGA). Small RNA-sequencing data was deposited on GEO (GSE57381).

Cells and reagents

Huh-7.5, FT3-7 (a clonal derivative of Huh7 cells), wild-type and Ago2 knockout murine embryonic fibroblasts (MEFs) were maintained as described previously (8,19). Sofosbuvir (2′-deoxy-2′-α-fluoro-β-C-methyluridine-5′-monophosphate) was obtained from CHEMSCENE, LLC. Final dilutions contained 0.1% dimethyl sulfoxide.

Plasmids

pH77S.3/GLuc, pH77S/GLuc-AAG, pHJ3-5/GLuc, pHJ3-5/GLuc-GND, pJFH1/GLuc, its cell culture-adapted variant, pJFH1-QL/GLuc, the related S1-, S2- and S1-S2-p6m mutants, and psiCHECK2/Luc-3′HCV have been described previously (8,19,29). Mutations

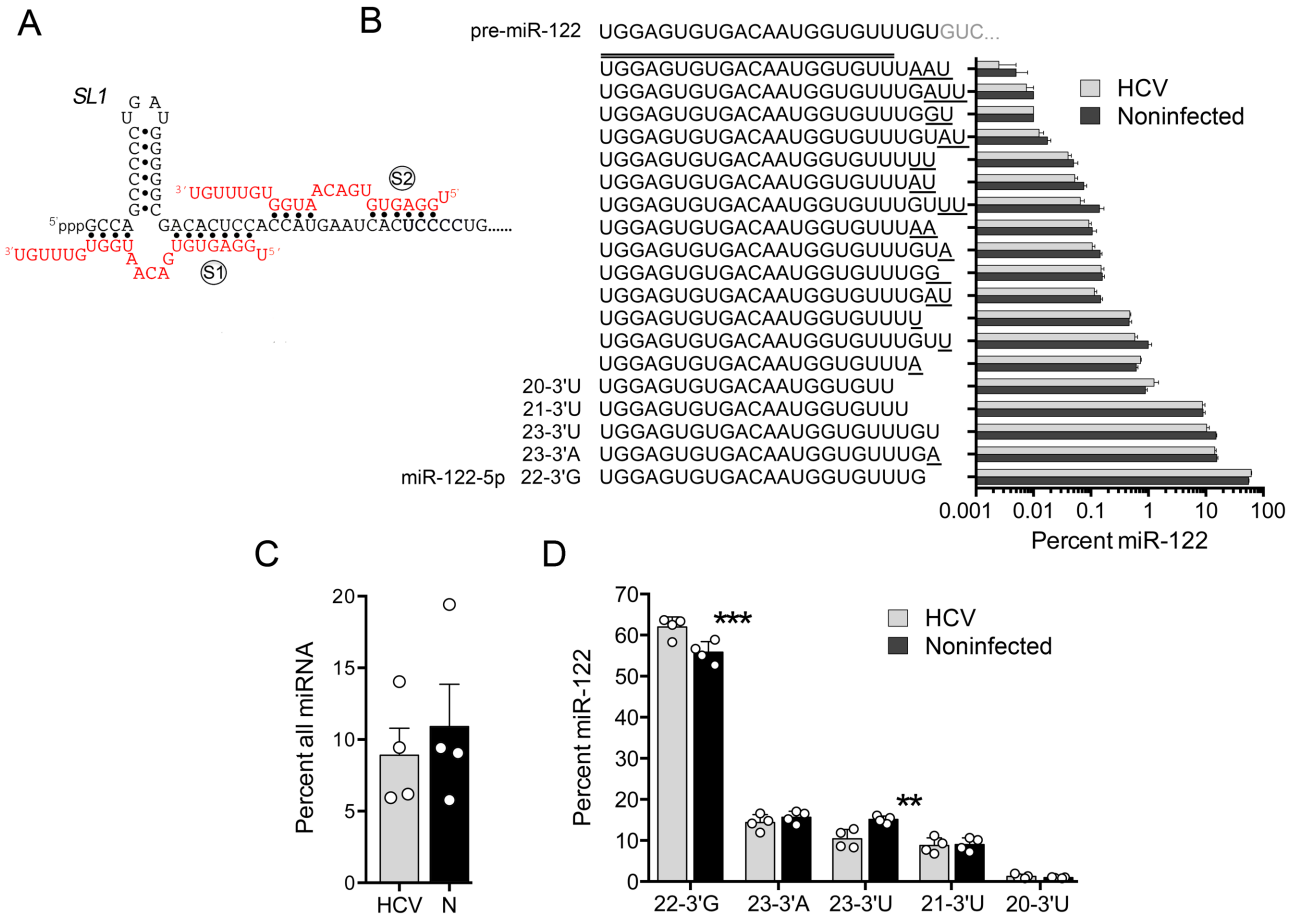

Figure 1. Natural variation in the 3′ terminal bases of the HCV host factor, miR-122. (**A**) Base-pair interactions between miR-122 (red font) and the extreme 5′ end of the positive-strand HCV RNA genome (black font) established in previous mutational analyses. (S1) and (S2) represent seed-match sites, *SL1* indicates stem-loop 1 in the HCV 5′UTR. Note the absence of base pairs involving the 3′ terminal 6 nucleotides of miR-122. (**B**) The 19 most abundant miR-122-5p (guide strand) variants identified in non-malignant liver tissue from HCV-infected and non-infected human subjects ($n = 4$ each). Sequences are listed according to their abundance (percent of all small RNAs sharing the core 5′ miR-122 sequence 'UGGAGUGUGACAAUGGUGUU'). Underlined bases represent non-templated additions and deletions. The pre-miR-122 sequence is shown at the top for comparison. Error bars represent the SEM. (**C**) Relative abundance of all miR-122 reads as the percentage of all miRNAs in HCV-infected (HCV) and non-infected (N) liver tissue. (**D**) Expanded view of the five most abundant miR-122 variants in HCV-infected versus non-infected human liver. Each symbol represents the result from an individual sample. Error bars represent SD, $n = 4$. $^{**}P < 0.01$, $^{***}P < 0.001$, by ANOVA with Holm-Sidak's multiple comparisons test.

or deletions in H77S/GLuc-AAG-S1p6m/dSL1 and -S1p6m/Ins5U mutants were introduced by primer-directed mutagenesis of the sequence spanning the NotI and AgeI sites as described (8). Single base substitutions were created within psiCHECK2/Luc-3′HCV by inserting pre-annealed oligonucleotides containing mutated sequences using the XhoI and NotI sites. The 3′UTR sequence of SLC7A1 containing natural miR-122 target sites (6) was amplified using SuperScript® III One-Step RT-PCR System with Platinum® Taq DNA Polymerase (Thermo Scientific) and primers 5′-AATTCTCGAGGACATAAGCTGT CTGGCCTCTCTGT-3′ and 5′-TTATATGCGGCCGC CTCAGTGGAACGCTCCACCCA-3′ from total RNA extracted from Huh-7.5 cells and cloned into psiCHECK2 using the XhoI and NotI sites. Base changes and the integrity of the surrounding sequences were confirmed by DNA sequencing.

RNA oligonucleotides

RNA oligonucleotides were synthesized by Dharmacon, and miRNAs were transfected as miRNA/miRNA* duplexes as described (19).

RNA transcription

RNA transcripts were synthesized *in vitro* as described previously (29).

Transfections

HCV RNA (5 μg) and duplex miRNA (250 pmol) were mixed with 5×10^6 FT3-7 or PH5CH8 cells in a 4-mm cuvette and pulsed once at 250 V, 950 μF and 50 Ω in a Gene Pulser Xcell Total System (Bio-Rad). MEFs were electroporated at 400 V, 250 μF and ∞ Ω.

Gaussia luciferase assay

Cell culture supernatant fluids were collected at intervals following transfection and cells then refed with fresh media. Secreted Gaussia luciferase (GLuc) activity was measured as described (29).

Immunoblots

Immunoblotting was carried out using standard methods with the following antibodies: mouse monoclonal antibodies (mAbs) to human Ago2 (Clone 1B1-E2H5, MBL International) or mouse Ago2 (Clone 2D4, Wako Chemicals); and rabbit monoclonal antibody to Ago2 (Cell Signaling Technology). Protein bands were visualized with an Odyssey Infrared Imaging System (Li-Cor Biosciences).

Ago2-RNA co-immunoprecipitation

Five million MEFs or FT3-7 cells were electroporated with 5 μg HCV RNA and 250 pmol duplex miRNAs and seeded onto a 10 cm dish. Five hours later, cells were harvested in lysis buffer [150 mM KCl, 25 mM Tris-HCl pH 7.4, 5 mM EDTA, 1% Triton X-100, 5 mM DTT, Complete protease inhibitor cocktail (Roche) and 100 U/ml RNaseOUT (Invitrogen)]. Lysates were centrifuged, and filtered through a 0.22 μm syringe filter. Filtrates were incubated with anti-mouse Ago2 mAb (Wako Chemicals), anti-human Ago2 mAb (MBL International) or isotype control IgG at 4°C for 2 h, followed by the addition of 30 μl of Protein G Sepharose (50% Slurry, GE Healthcare) for 1 h. The Sepharose beads were washed three times in wash buffer [1 × TBS, 1.2% Triton X-100, 5 mM DTT, Complete protease inhibitor cocktail (Roche), 80 U/ml RNaseOUT (Invitrogen)] and RNA extracted using the RNeasy Mini Kit (Qiagen). HCV RNA associated with Ago2 protein was quantified by cDNA synthesis using SuperScript® III First-Strand Synthesis SuperMix for qRT-PCR (Invitrogen) followed by TaqMan qPCR analysis using iQ Supermix (Bio-Rad), or measured semi-quantitatively by RT-PCR as described (19).

psiCHECK2 reporter assay

PH5CH8 cells or MEFs seeded on 96-well plates were co-transfected with 20 ng of psiCHECK2 DNA and 50 nM duplex miRNA using siLentFect™ Lipid Reagent (Bio-Rad). Twenty-four hours later, the cells were lysed in 30 μl of Passive Lysis Buffer (Promega). Firefly (FLuc) and Renilla luciferase (RLuc) reporter activities were measured using a Dual-Luciferase Reporter Assay System (Promega) (8).

CLEAR-CLIP data analysis

Previously described CLEAR (covalent ligation of endogenous Argonaute-bound RNAs)-CLIP sequence data from a study of HCV RNA-associated miRNAs (15) was retrieved from the NCBI Gene Expression Omnibus (GSE76967). Reads containing miR122 sequence fused at its 3′ end to sequence near the 5′ end of HCV RNA were extracted by filtering for nts 2–21 of the miR-122 sequence and the S1/S2 seed site sequences of HCV. miR-122 3′ end variants were enumerated and percentages calculated. Data were considered only from accessions in which >1000 such miR-122 reads were identified (SRX1534493, SRX1534494, SRX1534496, SRX1534497 and SRX1534500).

Statistical analyses

Unless noted otherwise, all between-group comparisons were carried out by one-way or two-way ANOVA using Prism 6.0 software (GraphPad Software, Inc.).

RESULTS

Relative expression of miR-122 variants in liver from HCV-infected versus non-infected individuals

Mature miRNAs, including miR-122, are subject to a variety of 3′ modifications, including non-templated adenylation, uridylation and trimming, that influence both their stability and function (27,30). We previously reported the use of high-throughput sequencing to profile in an unbiased fashion the expression of small non-coding RNAs in liver tissue collected from a series of Japanese adults with chronic viral hepatitis (31). To determine the relative abundance of different 3′ miR-122 variants in human liver, we re-analyzed data from eight of these subjects, four with chronic HCV infection and four non-infected control individuals undergoing resection of metastatic tumors. We identified between 258 000 and 738 000 individual reads in each sample that shared a common 5′ 20 nt miR-122 sequence (5′-UGGAGUGUGACAAUGGUGUU-3′) but had varied 3′ ends. The most abundant of these, a 22 nt RNA with a 3′ guanosine (the canonical miR-122-5p in miRBase, which we term '22–3′G' in this report) accounted for no more than 63% of all miR-122 reads in any one sample (Figure 1B). Although the proportion of all miRNAs comprised by miR-122 reads varied considerably between individual study subjects (Figure 1C), the relative abundance of the five most highly expressed variants of miR-122 (22–3′G, 23–3′A, 23–3′U, 21–3′U and 20–3′U) was remarkably constant (Figure 1D). Notable exceptions were 23–3′U, which represented a lower proportion of all miR-122 reads in HCV-infected compared to non-infected subjects, and 22–3′G, which was reciprocally increased (Figure 1D). These results are consistent with reductions in the percentage of 23–3′U isoforms of miR-122 recently described by Kim *et al*. (32) in a small number of HCV-infected individuals, although the reduction in 23–3′U was lesser in magnitude and not associated with an increase in 21–3′U reported in that study.

FT3-7 cells are derived from human hepatoma Huh-7 cells and are highly permissive for HCV infection (19). Using a similar high-throughput sequencing strategy, we found the overall pattern of expression of the 3′ miR-122 variants in these cells differed significantly from that in liver tissue. 22–3′G had a greater relative abundance, representing about 80% of all miR-122 reads, whereas 23–3′U and especially 23–3′A were reduced (Figure 2A). These differences were highly significant statistically. To determine whether the 3′ variants are equally capable of being loaded into Ago2, a central component of the miRISC complex, we also quantified their abundance in RNA extracted from an FT3-7 cell

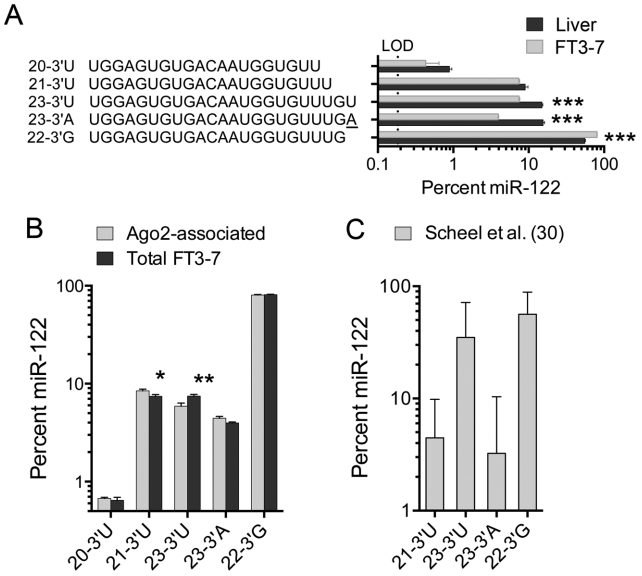

Figure 2. miR-122 3′ end variants expressed in a hepatoma cell line, FT3-7. (**A**) Relative abundance of the top five miR-122 variants expressed in FT3-7 cells compared to liver tissue. LOD = limit of detection (100 reads). ***$P < 0.001$ by two-way ANOVA with Holm-Sidak multiple comparisons test. (**B**) The five most abundant miR-122 variants are loaded into Ago2 with minimally different efficiencies. Error bars represent the SEM, $n =$ 3 independent cultures. *$P < 0.05$, **$P < 0.01$ by ANOVA with Holm-Sidak multiple comparisons test. (**C**) Relative abundance of the four major miR-122 3′ variants associated with HCV RNA in infected Huh-7 cells, as determined by a re-analysis of previously published CLEAR-CLIP data (15). A total of 19 129 miR-122 sequences with 3′ fusion to HCV 5′UTR RNA were characterized. Data shown are means ± SD; $n = 5$ experiments.

Ago2 immunoprecipitate (31). Although statistically significant, differences between their relative abundance in the Ago2 extract versus total cell lysate were small in magnitude and unlikely to be of biological importance (Figure 2B). Thus, the major 3′ miR-122 variants are loaded into Ago2 with only minor differences in efficiency.

To ascertain whether these 3′ miR-122 variants are recruited to replicating viral RNAs within infected human hepatoma cells, we analyzed CLEAR-CLIP sequencing data generated in a previously published study (15) in which Ago2-associated miRNAs were covalently ligated to their cellular and viral RNA targets in HCV-infected Huh-7.5 cells. We filtered these data to identify chimeric sequences in which miR-122 was fused at its 3′ end to HCV RNA containing the S1 and/or S2 sites near the 5′ end of the genome, and enumerated the different 3′ variants present. Although we found substantial variation in the distribution of the variants in different experiments, the overall proportions of each of the four major 3′ miR-122 variants did not differ significantly from what we had found in FT3-7 cells (Figure 2C). Thus, the minor 3′ variants are not only loaded into Ago2 complexes, they are also recruited to the 5′ end of HCV RNA in infected cells expressing an abundance of the canonical 22–3′G isoform.

Differential capacities of miR-122 variants to support HCV genome amplification

We next assessed the capacities of the 3′ miR-122 variants to support replication of an HCV RNA reporter genome (H77S.3/GLuc-S1-S2p6m) in Huh-7.5 cells (Figure 3A). This HCV reporter RNA contains A-to-U substitutions at each of the bases pairing with nucleotide 6 of miR-122 in the S1 and S2 seed match sites (Figure 3B). This prevents replication of the reporter RNA genome unless it is co-transfected with a complementary mutant duplex miR-122 mimic (designated 'miR-122p6') (7). Since replication of the genome can be monitored non-invasively by measuring GLuc activity secreted by transfected cells, this provides a simple system for assessing the capacity of miR-122p6 variants to support replication in cells expressing endogenous, wild-type miR-122. We thus co-transfected the reporter genome individually with duplex miR-122p6 mimics representing each of the four most abundant 3′ variants (22–3′G, 23–3′A, 23–3′U and 21–3′U, Figure 1A), and monitored secreted GLuc activity over the ensuing 72 h. As negative controls, we also co-transfected the reporter genome with miR-124, an unrelated brain-specific miRNA or wild-type miR-122 (23–3′U). In each case, we used duplex RNAs as mimics because the two-nucleotide 3′ overhang of mature miRNA is important for efficient loading of the guide strand into miRISC complexes.

Surprisingly, the most abundant 3′ miR-122p6 variant (22–3′G) was not the most active in facilitating amplification of the reporter virus genome (Figure 3C). Both of the 23 nt long miR-122p6 variants (23–3′U and 23–3′A) were 3–4 fold more efficient than 22–3′G variant in promoting replication, whereas the 21–3′U variant was completely inactive. Similar results were obtained with a second HCV RNA which, in contrast to the genotype 1a 5′UTR in the H77S.3/GLuc-S1-S2p6m reporter virus, contains the 5′UTR sequence of a genotype 2a virus, JFH1 (Supplementary Figure S1). These results suggest that either the length and/or the composition of the 3′ terminal nucleotides of miR-122 are important for its ability to support efficient HCV RNA replication. To distinguish between these possibilities, we tested a 23 nt miR-122p6 mutant in which the 3′ terminal nucleotides (nts 22 and 23) were substituted with complementary bases (23–3′CAp6). This miR-122 mimic did not function as well as either the 23–3′U or 23–3′A (Figure 3C). We conclude from these results that both the length and the composition of the 3′ terminal nucleotides of miR-122 are important for its HCV host factor activities.

We demonstrated previously that the ability of miR-122 to stabilize the HCV RNA genome and to promote its synthesis depends upon its recruitment of Ago2 to the viral 5′UTR (4,8). Thus, we next ascertained whether the differences we observed in the host factor activity of these 3′ miR-122 variants correlate with differences in their capacity to recruit Ago2 to the viral genome. To accomplish this, we immunoprecipitated Ago2 from lysates of cells co-transfected with HCV RNA and the miR-122 variants and then assessed the amount of HCV RNA associated with Ago2 using semi-quantitative RT-PCR. These experiments revealed that there was less viral RNA associated with Ago2 in cells transfected with the 22–3′G variant than the 23–3′U

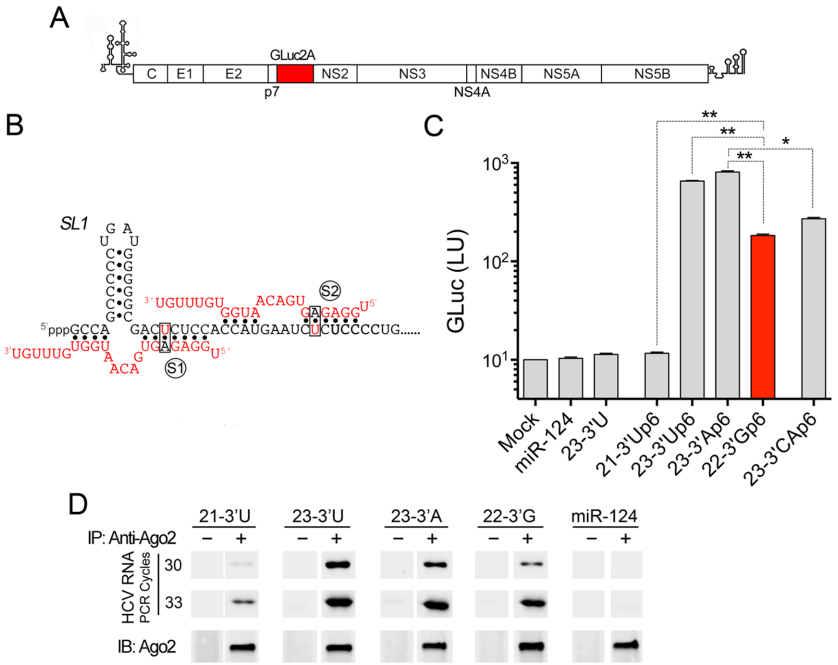

Figure 3. The capacity of miR-122 variants to promote HCV genome amplification correlates with their ability to bind HCV RNA as a complex with Ago2. (**A**) Schematic of the HCV GLuc reporter genome, showing insertion of GLuc2A sequence between the p7 and NS2 coding regions (see 'Materials and Methods' section). (**B**) Base-pair interactions between HCV RNA carrying p6m mutations in the miR-122 seed match sequences (black font, with red nucleotide substitution) and two copies of Ago2-associated miR-122p6 with complementary base substitutions (red font with black nucleotide substitution). (S1) and (S2) indicate seed-sequence interaction sites; *SL1* = stem-loop 1. (**C**) H77S.3/GLuc RNA containing double S1 and S2 p6m mutations were co-transfected into Huh-7.5 cells with the indicated wild-type or mutant duplex miR-122s or the control miRNA, miR-124. Data shown represent the GLuc activity secreted into media between 48 and 72 h post-transfection. 22–3′Gp6 is representative of the most abundant miR-122 variant (22–3′G, see Figure 1), and is shaded in red here and in subsequent figures. Selected pair-wise comparisons are shown: $*P < 0.05$, $**P < 0.01$ by one-way ANOVA with Dunnett's correction for multiple comparisons. Error bars represent SD; $n = 3$ technical replicates. Results shown are representative of multiple independent experiments with similar results (see also Supplementary Figure S1). (**D**) Semi-quantitative RT-PCR results of HCV RNA associated with Ago2 precipitated from lysates of murine embryonic fibroblast (MEFs) that had been co-electroporated with the non-replicating H77S.3/AAG RNA and either a miR-122 variant or the control miR-124. Immunoblots of immunoprecipitated Ago2 are shown in lower panels.

or 23–3′A variants, and very little HCV RNA associated with Ago2 isolated from 21–3′U-transfected cells (Figure 3D). These results correlate well with the HCV host factor activities of the 3′ miR-122 variants (Figure 3C and Supplementary Figure S1). Since the variants demonstrate similar efficiencies for loading into Ago2 (Figure 2B), these results suggest that the 3′terminal nucleotides of miR-122 play an important role in determining the affinity of the miR-122–Ago2 complex for the viral RNA. This conclusion stands in sharp contrast to the absence of any interactions between the 3′ terminal miR-122 nucleotides and HCV RNA in the model structures shown in Figures 1A and 3B.

3′ miR-122 variants differ in their capacity to stabilize HCV RNA and promote its replication in hepatocyte-derived cells lacking endogenous miR-122 expression

To exclude the possibility that the results described above might reflect aberrant miR-122 target site specificities related to the p6m mutations present in the reporter viruses, we carried out similar experiments in a second human hepatocyte-derived cell line. PH5CH8 cells are T antigen-transformed, non-neoplastic adult human hepatocytes. They have no detectable miR-122 expression, making HCV replication in these cells completely dependent upon transfection of exogenous miR-122 (33). We transfected PH5CH8 cells with a genotype 2a HCV reporter virus RNA similar to that shown in Figure 3A that contains the wild-type miR-122 seed-binding and downstream 5′UTR sequence (JFH1-QL/GLuc) together with duplex mimics of the various wild-type 3′ miR-122 variants. Negative miRNA controls for these experiments included duplex miR-122p6 or miR-124. As shown in Figure 4A, amplification of reporter virus RNA (marked by GLuc expression between 24–72 h post-transfection) was maximal when it was co-transfected with the 23–3′U or 23–3′A miR-122 variant. Co-transfection with 22–3′G resulted in significantly lower levels of replication ($P < 0.0001$), whereas co-transfection with 21–3′U completely failed to support replication (Figure 4A). These results thus mirror closely those described above from experiments in Huh-7.5 cells supplemented with p6 mutant versions of these 3′ miR-122 variants (Figure 3C), and thereby exclude any confounding effect of the p6 mutation. The 23–3′CA mutant was also demonstrably less active than 23–3′A and 23–3′U in promoting HCV replication in PH5CH8 cells ($P < 0.0001$ at 72 h), similar to the 23–3′CAp6 mutant in Huh-7.5 cells (Figure 3C).

In an effort to discern whether differences in the capacity of the 3′ miR-122 variants to support HCV genome amplification result from differences in stabilization of the transfected RNA versus differences in viral RNA synthesis, we

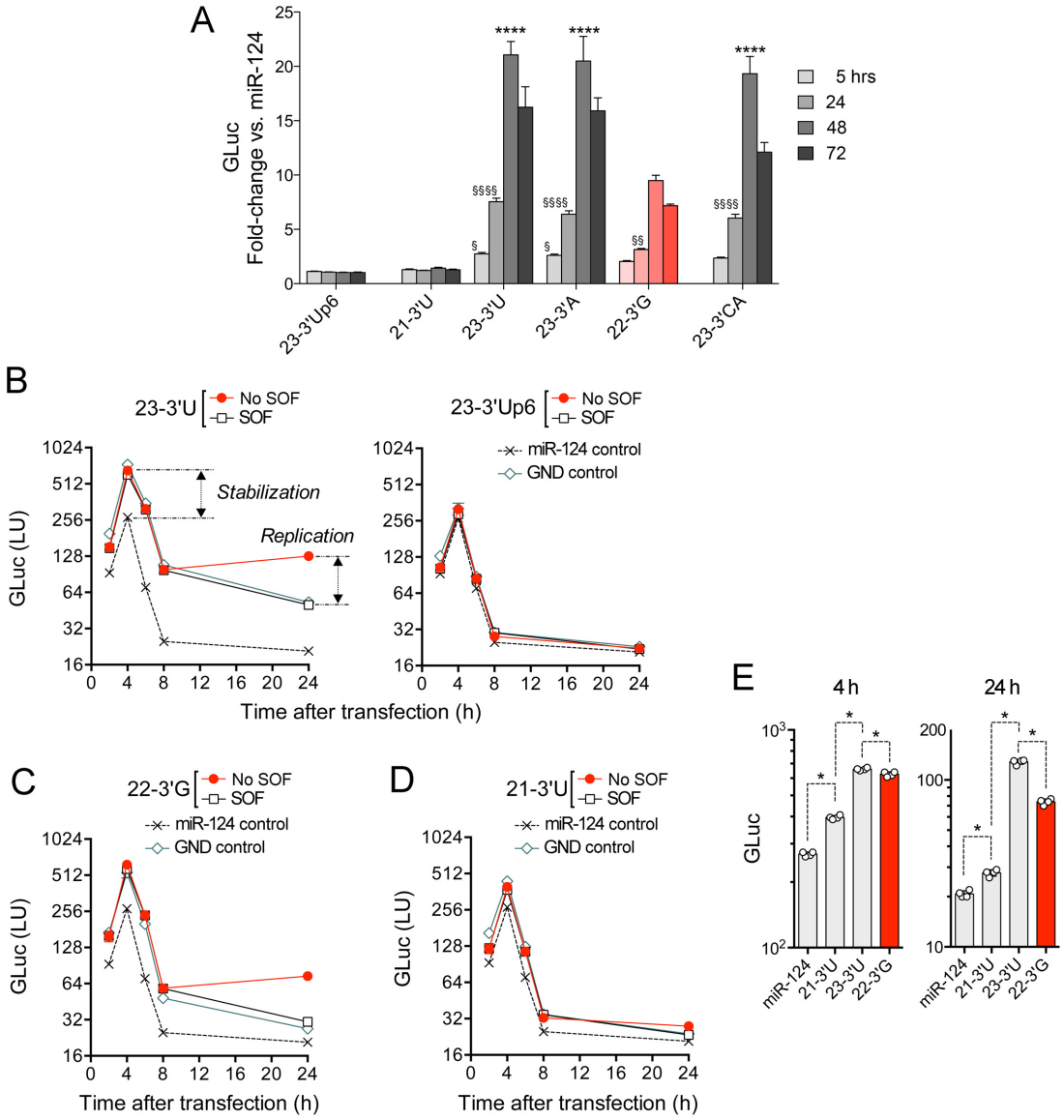

Figure 4. Capacity of natural miR-122 variants to promote stabilization and amplification of the HCV genome. (**A**) PH5CH8 cells were co-transfected with the replication competent, genome-length JFH1-QL/GLuc reporter virus RNA, which contains the wild-type HCV 5′UTR sequence and the indicated wild-type 3′ miR-122 variants. Supernatant fluids were collected at 5 h, and then 24 h intervals thereafter and assayed for GLuc activity. Results are presented as the fold-increase in GLuc relative to that in cells co-transfected with the control miRNA, miR-124. $^{****}P < 0.0001$ by two-way ANOVA for comparisons with the 22–3′G variant at 24, 48 and 72 h; $^{\S}P < 0.05$, $^{\S\S}P < 0.01$, $^{\S\S\S\S}P < 0.0001$ for comparisons with the miR-122 mutant 23–3′Up6 at the indicated time point. (**B**) PH5CH8 cells were co-electroporated with HCV JFH1/GLuc RNA and the (left) 23–3′U variant or (right) 23–3′Up6 mutant, then cultured in the presence or absence of the NS5B inhibitor sofosbuvir (SOF). As negative controls for viral RNA amplification, parallel cultures were co-electroporated with miR-124 or a non-replicating HCV RNA containing a lethal GND mutation in the NS5B polymerase. Secreted GLuc activity was followed at intervals. Similar experiments are shown involving transfection of (**C**) 22–3′G or (**D**) 21–3′U. (**E**) Comparison of 4 h (stabilization) and 24 h results (stabilization + replication) from the experiments shown in panels A–C. Symbols represent GLuc values from individual cultures. In all panels, error bars represent the SD from $n = 4$ technical replicates. $^{*}P = 0.03$ by two-sided Mann–Whitney test. Note that GLuc activity is shown on a log scale in each panel. The data shown are representative of two independent experiments.

carried out additional experiments assessing GLuc expression immediately following transfection of PH5CH8 cells. To distinguish GLuc expression resulting from genome replication versus translation of the transfected input RNA, we transfected cells with a reporter viral RNA containing a lethal mutation in the NS5B RNA polymerase (JFH1/GLuc-GND) that prevents viral RNA synthesis. We also cultured the cells in the presence or absence of sofosbuvir (SOF), a potent antiviral inhibitor of HCV replication. Secreted GLuc activity was measured at 2 h intervals up to 8 h post-transfection, and again at 24 h. Results from a typical experiment involving transfection of the 23–3′U variant are shown in Figure 4B (left). GLuc secreted between 2 and 8 h after transfection reflects translation of the input RNA (4,8,11,19), and was similar for both replication-competent and incompetent GND mutant RNAs. Our prior studies

and those of others show that miR-122-mediated increases in secreted GLuc activity at these early time points reflect largely if not entirely increased stability of the transfected RNA (8,11–12). Similar increases were observed in the presence of SOF, a potent inhibitor of replication (Figure 4B, left). Later miR-122-mediated increases in GLuc activity (24 h) reflect enhanced RNA replication in addition to stabilization, and were not observed with SOF treatment or in cells transfected with the GND mutant despite stabilization of the RNA (Figure 4B, left). These data thus reveal that 23–3′U both stabilizes the HCV RNA and enhances its replication (Figure 4B, left). In contrast, neither enhanced stability nor increased replication followed transfection of 23–3′Up6 or the irrelevant miRNA control, miR-124 (Figure 4B, right). Similar experiments confirmed that 22–3′G is active in both stabilizing the viral RNA as well as stimulating RNA synthesis (Figure 4C), albeit significantly less efficiently than 23–3′U (Figure 4E). In contrast, whereas the 21–3′U variant demonstrated a statistically significant capacity to stabilize the HCV RNA, this effect was much less than that observed with 23–3′U and 22–3′G (Figure 4D and E). Its ability to stimulate viral RNA synthesis was negligible (Figure 4D). These results are consistent with those obtained with the p6 miR-122 mutants in Huh-7.5 cells (Figure 3C) and the wild-type miR-122 variants in PH5CH8 cells (Figure 4A).

miRNA-induced miRISC activity of naturally occurring 3′ miR-122 variants

To determine whether the 3′ miR-122 variants differ in their capacity to form functionally active miRISC complexes, we co-transfected the variants into cells together with a reporter plasmid psiCHECK2 expressing an RLuc transcript that has the natural miR-122 SLC7A1 (a.k.a. CAT1) target sequence containing three miR-122 binding sites in its 3′UTR (6). RLuc activities were normalized to FLuc activity produced from a second, independent ORF expressed by the reporter plasmid. Interestingly, the four major miR-122 variants, including 21–3′U, demonstrated comparable suppressive activity when co-transfected with the reporter plasmid into MEFs (Figure 5A, left) or PH5CH8 cells (right), both of which do not express endogenous miR-122. In contrast, in many (but not all) experiments the 21–3′U variant was modestly less active than the other variants in suppressing expression of a reporter containing nts 1–45 of the HCV genome within its 3′UTR (Figure 5B). This trend was evident in both cell types, but statistically significant only in PH5CH8 cells. miR-122 suppression of the HCV reporter was entirely dependent on Ago2, because the 23–3′U variant had no effect on RLuc expressed from this reporter in genetically deficient *Ago2*$^{-/-}$ MEFs (Figure 5C). We conclude from these results that the 21–3′U variant is less active in targeting the HCV RNA sequence than the other major 3′UTR variants, although the magnitude of this difference is much less in reporter gene suppression assays (Figure 5) than in the HCV host factor assays described above (Figures 3C and 4A–D).

To ascertain whether the 21–3′U variant is less active in targeting one or the other of the two HCV seed match sites, we constructed additional reporter plasmids with a p6m mutation (Figure 3B) in either S1 or S2. When co-transfected with the S1-p6m reporter plasmid, wild-type miR-122 is directed to the S2 site and *vice versa*. Interestingly, the 21–3′U variant was incapable of suppressing RLuc expression from the HCV 3′UTR reporter in MEFs when directed to the S1 site, whereas it suppressed RLuc expression as efficiently as the other miR-122 variants when directed to the S2 site (Figure 5D). The 22 and 23 nt long variants had similar activities when directed to either S1 or S2. These results indicate that the 3′ terminal nucleotides of miR-122 are important for miR-122 to properly bind and recruit Ago2 to the S1 site, but that binding to the S2 site alone is largely sufficient for miRISC activity when the target sequence is placed in the 3′ UTR of a reporter construct.

The 3′ terminal nucleotides of miR-122 are required for recruiting Ago2 to the S1 site and essential for efficient promotion of HCV RNA replication

To confirm that the 21–3′U variant is deficient in targeting the S1 site in the context of genome-length HCV RNA, we carried out a series of Ago2-pulldown experiments. HCV RNAs containing the p6m substitution in either S1 or S2 were co-transfected into MEFs together with duplex miR-122p6 mimics containing a complementary p6 mutation. Since MEFs lack endogenous expression of miR-122 (8), we were able to assess the capacity of each variant to bind and recruit Ago2 to the viral RNA by quantifying the amount of HCV RNA present in Ago2 immunoprecipitates. Consistent with the results of the reporter assays, 21–3′Up6 failed to recruit Ago2 to the S1 site of the S1p6m RNA (Figure 6A, left), whereas it efficiently recruited Ago2 to the S2 site in the S2p6m RNA (right). This difference was highly significant statistically ($P = 0.710$ for miR-124 versus 21–3′U in the S1p6m-transfected cells, versus $P < 0.0001$ in the S2p6m-transfected cells, by two-way ANOVA).

We confirmed the inability of 21–3′U to interact with the S1 site by determining whether supplementing Huh-7.5 cells with 21–3′Up6 or 22–3′Gp6 promotes replication of HCV RNAs containing the p6m substitution in S1 or S2. These cells express endogenous miR-122 capable of interacting with the non-mutated seed match site in these RNAs, making replication of the RNA dependent upon the capacity of the transfected p6 mutant miR-122 to bind to the mutated S1 or S2 site. As anticipated, 21–3′Up6 promoted replication when directed to S2, but not S1, whereas 22–3′Gp6 promoted replication when directed to either site (Figure 6B). 22–3′Gp6 also stimulated replication of a double S1+S2p6m mutant RNA, whereas 21–3′Up6 did not. We validated these results using a HCV target genome with a different mutation in the S1 site involving the third nucleotide in the seed sequence binding region, ‘p3m’. A cognate 21–3′Up3 miR-122 variant had much weaker activity in promoting replication of this RNA than 23–3′Up3, confirming that the inability of 21–3′U to promote replication is not an artifact caused by the p6m substitution in the HCV genome (Supplementary Figure S2). Thus, the 21–3′U variant lacks HCV host factor activity because it has a reduced capacity to bind the S1 site and recruit Ago2 to it.

It is puzzling that 21–3′U should have less affinity for the S1 site than S2, as the seed match sequence in S1 is 7 nts long

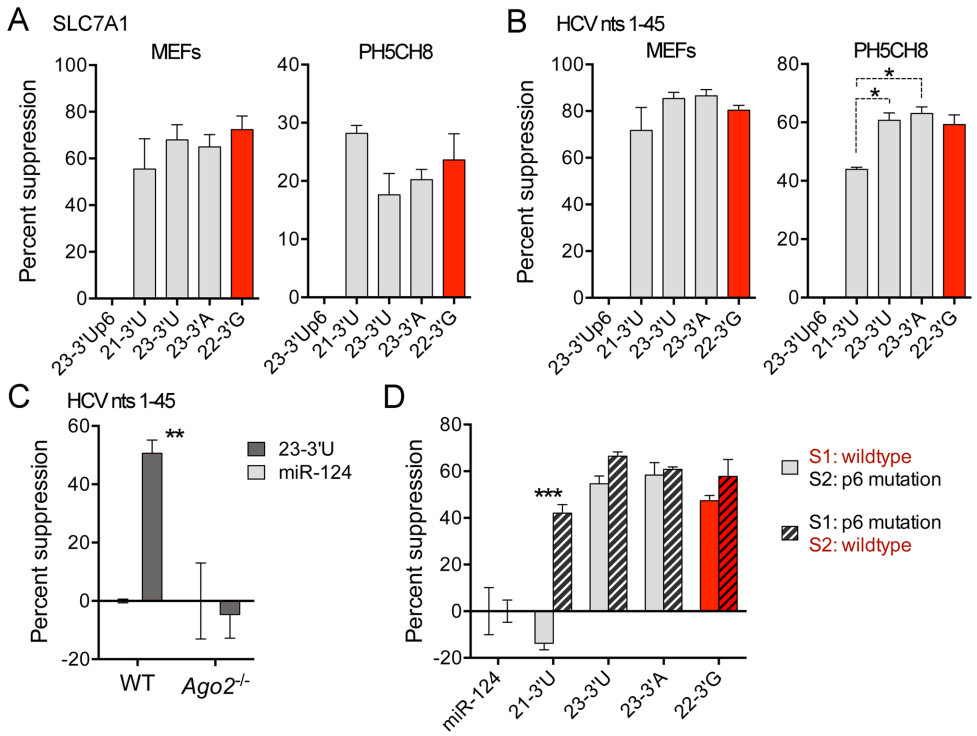

Figure 5. Capacity of miR-122 variants to suppress translation of RLuc expressed by a capped reporter mRNA containing (**A**) the natural SLC7A1 (CAT1) 3′UTR miR-122 target or (**B**) nts 1–45 of the HCV RNA genome in its 3′UTR. Experiments were carried out in MEFs (left panels) or PH5CH8 cells (right). Results are shown as percent suppression for each miR-122 variant relative to 23–3′Up6 that was included as a negative control. Error bars represent SEM from three independent experiments (2 for SLC7A1 tested in MEFs), each with 3–4 technical replicates. $*P < 0.05$ by one-way ANOVA with Dunnett's correction for multiple comparisons. (**C**) Suppression of RLuc translation was measured under the condition of (B) in wild-type or *Ago2*$^{-/-}$ MEFs. Error is the SEM of duplicate cultures. $**P < 0.01$ by two-sided *t*-test. (**D**) MEFs were co-transfected with psiCHECK2 expressing RLuc reporter mRNA transcripts containing in their 3′UTR the HCV miR-122 target sequence (HCV nts 1–45) with p6m mutations (Figure 3A) in either the S1 or S2 site, and either a miR-122 variant or miR-124. miR-122 was directed to the wild-type binding site (red font) in these experiments. Results were normalized to FLuc activity expressed from a different open reading frame in the same DNA. Error bars represent the SEM of triplicate cultures. $***P = 0.0002$ for wild-type S1 versus S2 seed match site, by two-way ANOVA with Sidak's correction for multiple comparisons.

whereas it is only 6 nts long in S2 (Figure 1A). However, structural studies of Ago2 complexed with a 21 nt guide RNA have revealed that nts 13–16 of the RNA are exposed for target recognition as well as nts 2–8 (the seed region) (34). Furthermore, base pairs involving nucleotides 3′ of the seed contribute substantially to miR-122 binding at both S1 and S2 (19). Although this region of the miR-122 guide strand (nts 13–17) is constant in the 3′ variants we studied, the upstream HCV nucleotides at the S2 site ('…CCAU…') provide for four Watson–Crick accessory pairs, whereas sequence upstream of S1 ('GCCA…') provides for only three with a possible additional wobble G-U pair (Figure 1A). To exclude a role for this difference in the lesser affinity of 21–3′U for the S1 site, we created a '…CCAU…' sequence upstream of the S1 seed match similar to that upstream of S2 by inserting a U at nt 5 of the HCV genome. This did not result in Ago2 recruitment to S1 by 21–3′U (Supplementary Figure S3A). We also considered the possibility that the binding of 21–3′U to the S1 might be compromised by a stable stem-loop (SL1) in the HCV sequence that exists between the seed match sequence and upstream HCV nucleotides that are known to form 3′ auxiliary base-pair interactions with miR-122 (19) (Figure 1A). However, removal of the stem-loop did not rescue recruitment of Ago2 to the S1 site by 21–3′U (Supplementary Figure S3B).

Collectively, these results reveal that significant difference exist in the targeting of the 21–3′U variant to the S1 versus the S2 site in the HCV RNA. Changes in the 3′ terminal nucleotide of 22 nt long miR-122 variants also conferred substantial differences in HCV host factor activity when targeted to S1 but not the S2 site. Replacing the 3′ terminal 22G nucleotide with adenosine (22–3′Ap6), uridine (22–3′Up6) or especially cytidine (22–3′Cp6) markedly reduced the capacity of the 22–3′Gp6 variant to promote replication of either H77S.3 or HJ3-5 RNAs containing p6m mutations at both sites (Figure 6C and Supplementary Figure S4A). However, this difference was noted only when the 22 nt variant was targeted to the S1 site, as 22–3′Cp6 promoted RNA replication as well as 22–3′Gp6 directed to S2 (Figure 6D). In contrast, when we replaced the 3′ terminal U of 23–3′Up6 with guanosine, there was no reduction in its capacity to promote HCV RNA replication (Supplementary Figure S4B). This demonstrates that it is the guanosine residue at nt 22 of miR-122 that is important, not the presence of a guanosine at the 3′ terminal position.

Collectively, these results show that the capacity of miR-122 to facilitate the replication of HCV is strongly dependent upon both its length and the presence of a guanosine at nt 22, with length being a more important factor.

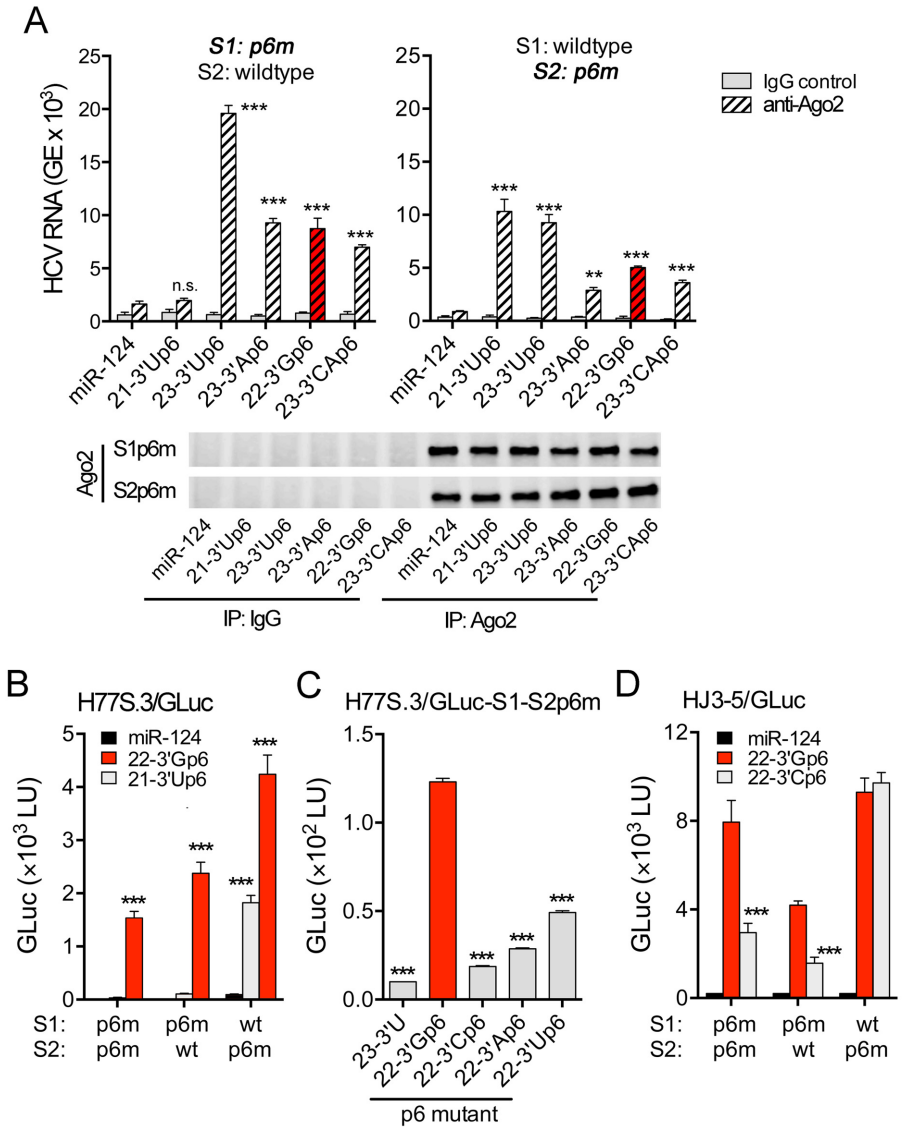

Figure 6. Length and composition of miR-122 3′ terminal nucleotides are important for recruiting an Ago2 complex to the S1 site in the HCV 5′UTR. (**A**) Ago2 complexed with the 21–3′U miR-122 binds S2 but not S1. Lysates were prepared from wild-type MEFs co-electroporated with (left) H77S/S1p6m/AAG or (right) H77S/S2p6m/AAG RNA mixed with miR-122p6 variants, and immunoprecipitated with anti-Ago2 antibody. Ago2-associated HCV RNA was quantified with quantitative RT-PCR. Error is the SEM of triplicate experiments. Immunoblots of immunoprecipitated Ago2 are shown below. Results versus miR-124: $^{**}P < 0.01$, $^{***}P < 0.001$ by one-way ANOVA with Dunnett's test for multiple comparisons. n.s. = not-significant. (**B**) H77S.3/GLuc RNAs bearing either single or double S1 and S2 p6m mutations were co-transfected with the indicated duplex miRNAs. Error is the SD of triplicate cultures. $^{***}P < 0.001$ versus miR-124 by two-way ANOVA with Holm-Sidek's multiple comparisons test. (**C**) H77S.3/GLuc RNA bearing double S1 and S2 p6m mutations was co-transfected with 22–3′Gp6 or similar 22 nt long RNA with either C, A or U at nt 22. Similar results were obtained with HJ3-5/GLuc RNA which contains genotype 2a sequence in the 5′ UTR (see Supplementary Figure S4A). $^{***}P < 0.001$ by one-way ANOVA with Dunnett's test for multiple comparisons. (**D**) HJ3-5/GLuc RNAs bearing either single or double S1 and S2 p6m mutations were co-transfected with the indicated duplex miRNAs. $^{***}P < 0.001$ versus 22–3′G by two-way ANOVA with Dunnett's multiple comparison test. (B–D) GLuc activity secreted into media between 48–72 h post-transfection is shown. Error bars represent the SD of triplicate cultures.

DISCUSSION

Recent studies indicate that the 3′-terminal nucleotides of miRNAs can contribute to target site selection, either by direct base-pair formation with the target RNA or by modulating key interactions of the miRNA with the PAZ domain of Ago (23–24,26). The 3′ terminal sequences of miRNAs are often modified by non-templated additions and deletions and, as we show here, miR-122 variants with non-canonical 3′ end sequence are abundant in human liver (Figure 1). *In vitro*, 22–3′G is the only product generated by Dicer cleavage of pre-miR-122, with the 23–3′A variant generated subsequently via engagement of the non-canonical cytoplasmic poly(A) RNA polymerase GLD2 (27). 23–3′A is likely to be more stable than 22–3′G (35), potentially contributing to its abundance. 22–3′G (and possibly 23–3′A) is also subject to trimming to shorter variants as well as 3′ uridylation mediated by terminal uridyl transferases (TUTases) (30). Whether these events occur prior to or following

dissociation of passenger strand RNA from newly formed miRISC complexes remains uncertain, although the GLD2 polymerase is more active on a single-strand substrate suggesting it may act after passenger strand loss (27).

CLEAR-CLIP studies have suggested that the 3′ terminal nucleotides of miR-122 influence its selection of mRNA targets in Huh-7 cells (26), but whether differences in the 3′ sequence also affect HCV host factor activity has not been studied. Our results suggest several important conclusions. The first is that there is a substantial, previously unrecognized difference in the structural and sequence requirements for miR-122 to function optimally as an HCV replication factor versus its canonical role in regulating host gene expression. Both the length and base composition of the 3′ end of miR-122 is critically important in determining its ability to promote HCV replication, but not gene regulation. This is evidenced by the fact that the 21–3′U isoform loads into Ago2 and functions in suppressing gene expression (Figures 2B, 5A and B), but fails to promote HCV replication (Figures 3C and 4D and E; Supplementary Figure S1). A related but equally important conclusion is that the current model of the interaction of miR-122 with HCV RNA (Figure 1A) is incomplete, as it offers no explanation for the requirement that miR-122 be at least 22 nts in length with a guanosine at position 22 (Figure 6C and Supplementary Figure S4A). While we do not fully understand the molecular basis for these requirements, we have shown that it centers on the inability of miR-122 isoforms lacking these criteria to functionally bind the S1 site that plays the major role in driving genome replication. A third major conclusion is that HCV replication is likely driven to a substantial extent by a minor 3′ miR-122 variant, 23–3′U. A review of previously described Ago2 CLEAR-CLIP data from HCV-infected cells (15) suggests that 23–3′U comprises about 26% of endogenously expressed miR-122 isoforms binding the 5′ end of the viral RNA, whereas the major, canonical 22–3′G isoform represents about 63% (Figure 2C). Since the 23–3′U variant is ∼3-fold as active as 22–3′G in promoting HCV replication (Figures 3C, 4E and Supplementary Figure S1), both variants likely contribute equivalently to HCV replication.

miR-122 promotes the replication of HCV by two distinct mechanisms. First, by binding to the S1 and S2 sites in association with Ago2, miR-122 physically stabilizes the RNA, slowing its rate of decay by protecting it from the major cytoplasmic 5′ exoribonuclease, Xrn1 (8,11–12,36). A number of studies have also suggested that miR-122 might act to enhance HCV IRES-directed translation (9,18,37–38). However, it is difficult to distinguish the impact of enhanced RNA template stability from greater IRES efficiency in driving increases in viral protein expression, particularly in biologically relevant cell-based studies using full-length, replication-competent viral RNAs. When protection from Xrn1-mediated 5′ HCV RNA decay is carefully controlled for, we and others have concluded that most if not all miR-122-driven increases in protein translation are due to enhanced RNA template stability (4,12–13). We have shown recently that miR-122 directly stimulates the synthesis of HCV RNA within infected cells as measured by increases in the rate of incorporation of 5-ethynyl uridine into nascent HCV RNA (13). Notably, this occurs in the absence of any increase in [^{35}S]-Met incorporation into nascent viral protein (13).

Although miR-122-mediated stabilization of HCV RNA and increased viral RNA synthesis are antithetical to the typical actions of miRNAs in downregulating host gene expression, both of these actions are dependent upon Ago2 (8–9,13). Previous studies have suggested that the recruitment of Ago2 to the viral RNA by miR-122 follows a canonical pattern of miRNA binding at both the S1 and S2 sites (17–19), with targeting dependent upon both the seed sequence (nt 2–8) of the guide strand as well as supplementary base pairs involving nts 13–16 that often stabilize miRNA target interactions to repress translation and destabilize mRNAs (34,39–40). Current models for the interactions of miR-122 with the 5′ end of the viral RNA, such as that shown in Figure 1A (17–19), thus show most of the 5′ 40 nucleotides of HCV RNA to be engaged in base pairing, either with other HCV bases in stem-loop 1 (SL1), or in interactions with one of two copies of miR-122. These models predict no involvement of the 3′ terminal 5–7 nts of miR-122 (Figure 1A). Thus, it is surprising that only miR-122 species equal to or longer than 22 nucleotides support HCV replication (Figure 3C), and that there is a strong preference for the canonical guanosine at nt 22 (Figures 3C, 6C and Supplementary Figure S4A), as we show here.

Our data demonstrate that nts 22–23 of miR-122 play a key role in binding to and recruiting Ago2 to the S1 site within the HCV genome (Figure 6A), as well as to the S1 site in mRNA reporter transcripts containing nts 1–45 of HCV RNA within their 3′UTR (Figure 5D). In contrast, Ago2-targeting to the S2 site was not sensitive to changes in either the length or composition of the 3′ terminal nucleotides of miR-122. While 3′ adenylation can increase the physical stability of miR-122 (27), reduced stability cannot explain the selective absence of HCV host factor activity associated with the 21–3′U variant as it was fully functional in suppressing RLuc expression from reporter mRNAs containing its native SLC7A1 3′UTR target sequence (Figure 5A). These data also exclude insufficient transfection as an explanation for the failure of 21–3′U to support HCV genome replication. The S1-site specific nature of the 21–3′U variant also argues against the notion that variation in the length and composition of the 3′ nts 22–23 is simply affecting the stability of miR-122 (Figures 5D and 6A).

The binding of miR-122 to S1 is dominant over S2 in facilitating HCV RNA replication (7,12,19). Thus, substitutions that ablate miR-122 binding to S1 have a more severe impact on replication than those that ablate binding to S2, which is in quantitative agreement with the two-fold greater abundance of RNA pulled down by antibody to Ago2 when miR-122 is directed to the S1 rather than the S2 site (Figure 6A). This is consistent with the fact that S1 contains a 7 base seed-match site that base-pairs with nts 2–8 of miR-122 as well as an adenosine nucleotide opposite miR-122 nt 1 that is likely to increase the affinity to Ago2 (34). In contrast, S2 has a shorter, 6 base seed-match target that pairs with nts 2–7 of miR-122. Thus, a greater affinity for Ago2–miR-122 complex formation at the S1 site is likely to be the basis for its dominance over S2. This may explain why the inability of the 21–3′U variant to recruit Ago2 to S1 (Fig-

ure 6), despite its efficient loading into Ago2 (Figure 2B), is so severely detrimental to its functions in stabilizing and promoting replication of HCV RNA. This dominance of complex formation at S1 over S2 is not evident in miR-122 suppression of reporter mRNA transcripts containing the HCV target sequence within their 3′ UTR. Although the S1 site also fails to bind 21–3′U when placed in the 3′UTR of such transcripts (Figure 5D), 21–3′U demonstrated surprisingly little diminution in its miRISC activity in these assays (Figure 5A and B).

Our findings stand in contrast to a previous report describing cell-free biophysical experiments that suggested miR-122 binds with greater affinity at the S2 site than at S1 (20). These studies examined interactions between RNA representing the 5′UTR of HCV and miR-122 guide molecules in the absence of Ago2 and other cellular RNA binding proteins in a reconstituted *in vitro* system, and yielded very different results from what we observed in our cell-based system. Whereas we found that 21–3′U failed to bind and recruit Ago2 to the S1 site (Figure 6A), a 19 nt miR-122 mutant (Δ20–23) appeared capable of functionally binding to both S1 and S2 *in vitro* (20). This difference highlights the potential importance of Ago2, which was absent in the *in vitro* studies, in miR-122 target selection.

Although binding to the S1 site is dominant in the host factor activity of miR-122, the miRNA has a greater impact on replication when bound to both tandem sites than when bound to either alone (10,12,19). Recent studies of the binding of miRNAs to closely spaced target sites show that the shuttling of an Ago2–miRNA complex between neighboring sites on a single RNA molecule synergistically promotes Ago2 retention time during initial interactions with the target RNA, providing a mechanism by which RNAs containing adjacent miRNA binding sites may function as potent miRNA sponges (16,23). Importantly, dynamic interactions between the 3′ end of the guide strand and the Argonaute protein PAZ domain can have a substantial influence on this process, potentially regulating Ago2 shuttling between adjacent target sites (23,41). In an effort to determine whether anchoring of the 3′ terminal nucleotides in the PAZ domain plays a distinct role in miR-122 target selection at S1 versus S2, we biotinylated 23–3′Up6 at its 3′ end, a modification that should disrupt such anchoring. This 3′ biotinylated miR-122 failed to promote HCV RNA replication when directed to either the S1 or S2 site, and it had very little activity in suppressing translation of reporter RNA transcripts containing either the HCV or SLC7A1 target sequences in their 3′UTR (data not shown). However, the fact that the 21–3′U-Ago2 complex selectively fails to be recruited to S1 in the absence of a functional S2 site (Figures 5D and 6A) argues against this resulting from a defect in lateral diffusion between the two sites.

In summary, the HCV host factor activity of miR-122 entails a strict requirement for a length of at least 22 nts and a preference for guanosine at nt 22 for functional targeting of the S1 site in the RNA genome of HCV. Why this is so remains enigmatic. Although the preference for guanosine at nt 22 suggests the possibility of specific base-pairing, this is not represented by any existing model of the complex formed by the viral genome and miR-122, nor is there any obvious nucleotide in the HCV sequence with which it might pair. Unfortunately, past efforts to characterize the structure of the S1 site in the presence and absence of miR-122 using SHAPE have not yielded clear results (20,21), and thus shed no light on this possibility. Both the length of miR-122 and the presence or absence of G-22 could influence tethering of the 3′ miRNA tail within the PAZ domain of Ago, which could be important for target site selection (24), but an influence on interactions with a yet-to-be discovered RNA-binding protein acting in concert with Ago2 cannot be excluded. The unique 3′ base composition and length required for miR-122 HCV host factor activity is likely to be explained only by a high resolution structural analysis of the HCV RNA–miR-122-Ago2 ternary complex.

SUPPLEMENTARY DATA

Supplementary Data are available at NAR Online.

ACKNOWLEDGMENT

The authors are grateful to Scott Hammond and Troels Scheel as well as members of the Lemon laboratory for helpful discussions.

FUNDING

National Institutes of Health [R01-AI095690, R01-CA164029 to S.M.L., in part]; University of North Carolina Cancer Research Fund (in part). Funding for open access charge: National Institutes of Health.
Conflict of interest statement. None declared.

REFERENCES

1. Westbrook,R.H. and Dusheiko,G. (2014) Natural history of hepatitis C. *J. Hepatol.*, **61**, S58–S68.
2. Yamane,D., McGivern,D.R., Masaki,T. and Lemon,S.M. (2013) Liver injury and disease pathogenesis in chronic hepatitis C. *Curr. Top. Microbiol. Immunol.*, **369**, 263–288.
3. Scheel,T.K. and Rice,C.M. (2013) Understanding the hepatitis C virus life cycle paves the way for highly effective therapies. *Nat. Med.*, **19**, 837–849.
4. Li,Y., Yamane,D., Masaki,T. and Lemon,S.M. (2015) The yin and yang of hepatitis C: synthesis and decay of hepatitis C virus RNA. *Nat. Rev. Microbiol.*, **13**, 544–558.
5. Jopling,C.L., Yi,M., Lancaster,A.M., Lemon,S.M. and Sarnow,P. (2005) Modulation of hepatitis C virus RNA abundance by a liver-specific microRNA. *Science*, **309**, 1577–1581.
6. Chang,J., Nicolas,E., Marks,D., Sander,C., Lerro,A., Buendia,M.A., Xu,C., Mason,W.S., Moloshok,T., Bort,R. *et al.* (2004) miR-122, a mammalian liver-specific microRNA, is processed from hcr mRNA and may downregulate the high affinity cationic amino acid transporter CAT-1. *RNA Biol.*, **1**, 106–113.
7. Jangra,R.K., Yi,M. and Lemon,S.M. (2010) Regulation of hepatitis C virus translation and infectious virus production by the microRNA miR-122. *J. Virol.*, **84**, 6615–6625.
8. Shimakami,T., Yamane,D., Jangra,R.K., Kempf,B.J., Spaniel,C., Barton,D.J. and Lemon,S.M. (2012) Stabilization of hepatitis C virus RNA by an Ago2-miR-122 complex. *Proc. Natl. Acad. Sci. U.S.A.*, **109**, 941–946.
9. Wilson,J.A., Zhang,C., Huys,A. and Richardson,C.D. (2011) Human Ago2 is required for efficient miR-122 regulation of HCV RNA accumulation and translation. *J. Virol.*, **85**, 2342–2350.
10. Jopling,C.L., Schutz,S. and Sarnow,P. (2008) Position-dependent function for a tandem microRNA miR-122-binding site located in the hepatitis C virus RNA genome. *Cell Host Microbe*, **4**, 77–85.

11. Li,Y., Masaki,T., Yamane,D., McGivern,D.R. and Lemon,S.M. (2013) Competing and noncompeting activities of miR-122 and the 5′ exonuclease Xrn1 in regulation of hepatitis C virus replication. *Proc. Natl. Acad. Sci. U.S.A.*, **110**, 1881–1886.
12. Thibault,P.A., Huys,A., Amador-Canizares,Y., Gailius,J.E., Pinel,D.E. and Wilson,J.A. (2015) Regulation of hepatitis C virus genome replication by Xrn1 and microRNA-122 binding to individual sites in the 5′ untranslated region. *J. Virol.*, **89**, 6294–6311.
13. Masaki,T., Arend,K.C., Li,Y., Yamane,D., McGivern,D.R., Kato,T., Wakita,T., Moorman,N.J. and Lemon,S.M. (2015) miR-122 stimulates hepatitis C virus RNA synthesis by altering the balance of viral RNAs engaged in replication versus translation. *Cell Host Microbe*, **17**, 217–228.
14. Janssen,H.L., Reesink,H.W., Lawitz,E.J., Zeuzem,S., Rodriguez-Torres,M., Patel,K., van der Meer,A.J., Patick,A.K., Chen,A., Zhou,Y. *et al.* (2013) Treatment of HCV infection by targeting microRNA. *N. Engl. J. Med.*, **368**, 1685–1694.
15. Scheel,T.K., Luna,J.M., Liniger,M., Nishiuchi,E., Rozen-Gagnon,K., Shlomai,A., Auray,G., Gerber,M., Fak,J., Keller,I. *et al.* (2016) A broad RNA virus survey reveals both miRNA dependence and functional sequestration. *Cell Host Microbe*, **19**, 409–423.
16. Luna,J.M., Scheel,T.K., Danino,T., Shaw,K.S., Mele,A., Fak,J.J., Nishiuchi,E., Takacs,C.N., Catanese,M.T., de Jong,Y.P. *et al.* (2015) Hepatitis C virus RNA functionally sequesters miR-122. *Cell*, **160**, 1099–1110.
17. Machlin,E.S., Sarnow,P. and Sagan,S.M. (2011) Masking the 5′ terminal nucleotides of the hepatitis C virus genome by an unconventional microRNA-target RNA complex. *Proc. Natl. Acad. Sci. U.S.A.*, **108**, 3193–3198.
18. Roberts,A.P., Lewis,A.P. and Jopling,C.L. (2011) miR-122 activates hepatitis C virus translation by a specialized mechanism requiring particular RNA components. *Nucleic Acids Res.*, **39**, 7716–7729.
19. Shimakami,T., Yamane,D., Welsch,C., Hensley,L., Jangra,R.K. and Lemon,S.M. (2012) Base pairing between hepatitis C virus RNA and microRNA 122 3′ of its seed sequence is essential for genome stabilization and production of infectious virus. *J. Virol.*, **86**, 7372–7383.
20. Mortimer,S.A. and Doudna,J.A. (2013) Unconventional miR-122 binding stabilizes the HCV genome by forming a trimolecular RNA structure. *Nucleic Acids Res.*, **41**, 4230–4240.
21. Pang,P.S., Pham,E.A., Elazar,M., Patel,S.G., Eckart,M.R. and Glenn,J.S. (2012) Structural map of a microRNA-122: hepatitis C virus complex. *J. Virol.*, **86**, 1250–1254.
22. Li,Y., Masaki,T., Shimakami,T. and Lemon,S.M. (2014) hnRNP L and NF90 interact with hepatitis C virus 5′-terminal untranslated RNA and promote efficient replication. *J. Virol.*, **88**, 7199–7209.
23. Chandradoss,S.D., Schirle,N.T., Szczepaniak,M., MacRae,I.J. and Joo,C. (2015) A dynamic search process underlies microRNA targeting. *Cell*, **162**, 96–107.
24. Hur,J.K., Zinchenko,M.K., Djuranovic,S. and Green,R. (2013) Regulation of Argonaute slicer activity by guide RNA 3′ end interactions with the N-terminal lobe. *J. Biol. Chem.*, **288**, 7829–7840.
25. Wang,Y., Juranek,S., Li,H., Sheng,G., Wardle,G.S., Tuschl,T. and Patel,D.J. (2009) Nucleation, propagation and cleavage of target RNAs in Ago silencing complexes. *Nature*, **461**, 754–761.
26. Moore,M.J., Scheel,T.K., Luna,J.M., Park,C.Y., Fak,J.J., Nishiuchi,E., Rice,C.M. and Darnell,R.B. (2015) miRNA-target chimeras reveal miRNA 3′-end pairing as a major determinant of Argonaute target specificity. *Nat. Commun.*, **6**, 8864.
27. Katoh,T., Sakaguchi,Y., Miyauchi,K., Suzuki,T., Kashiwabara,S. and Baba,T. (2009) Selective stabilization of mammalian microRNAs by 3′ adenylation mediated by the cytoplasmic poly(A) polymerase GLD-2. *Genes Dev.*, **23**, 433–438.
28. Spaniel,C., Honda,M., Selitsky,S.R. and Yamane,D. (2013) microRNA-122 abundance in hepatocellular carcinoma and non-tumor liver tissue from Japanese patients with persistent HCV versus HBV infection. *PLoS One*, **8**, e76867.
29. Yamane,D., McGivern,D.R., Wauthier,E., Yi,M., Madden,V.J., Welsch,C., Antes,I., Wen,Y., Chugh,P.E., McGee,C.E. *et al.* (2014) Regulation of the hepatitis C virus RNA replicase by endogenous lipid peroxidation. *Nat. Med.*, **20**, 927–935.
30. Ren,G., Chen,X. and Yu,B. (2014) Small RNAs meet their targets: when methylation defends miRNAs from uridylation. *RNA Biol.*, **11**, 1099–1104.
31. Selitsky,S.R., Baran-Gale,J., Honda,M., Yamane,D., Masaki,T., Fannin,E.E., Guerra,B., Shirasaki,T., Shimakami,T., Kaneko,S. *et al.* (2015) Small tRNA-derived RNAs are increased and more abundant than microRNAs in chronic hepatitis B and C. *Sci. Rep.*, **5**, 7675.
32. Kim,G.W., Lee,S.H., Cho,H., Kim,M., Shin,E.C. and Oh,J.W. (2016) Hepatitis C virus core protein promotes miR-122 destabilization by inhibiting GLD-2. *PLoS Path.*, **12**, e1005714.
33. Dansako,H., Yamane,D., Welsch,C., McGivern,D.R., Hu,F., Kato,N. and Lemon,S.M. (2013) Class A scavenger receptor 1 (MSR1) restricts hepatitis C virus replication by mediating toll-like receptor 3 recognition of viral RNAs produced in neighboring cells. *PLoS Path.*, **9**, e1003345.
34. Schirle,N.T., Sheu-Gruttadauria,J. and MacRae,I.J. (2014) Structural basis for microRNA targeting. *Science*, **346**, 608–613.
35. Burns,D.M., D'Ambrogio,A., Nottrott,S. and Richter,J.D. (2011) CPEB and two poly(A) polymerases control miR-122 stability and p53 mRNA translation. *Nature*, **473**, 105–108.
36. Li,Y., Yamane,D. and Lemon,S.M. (2015) Dissecting the roles of the 5′ exoribonucleases Xrn1 and Xrn2 in restricting hepatitis C virus replication. *J. Virol.*, **89**, 4857–4865.
37. Henke,J.I., Goergen,D., Zheng,J., Song,Y., Schuttler,C.G., Fehr,C., Junemann,C. and Niepmann,M. (2008) microRNA-122 stimulates translation of hepatitis C virus RNA. *EMBO J.*, **27**, 3300–3310.
38. Roberts,A.P., Doidge,R., Tarr,A.W. and Jopling,C.L. (2014) The P body protein LSm1 contributes to stimulation of hepatitis C virus translation, but not replication, by microRNA-122. *Nucleic Acids Res.*, **42**, 1257–1269.
39. Bartel,D.P. (2009) MicroRNAs: target recognition and regulatory functions. *Cell*, **136**, 215–233.
40. Wee,L.M., Flores-Jasso,C.F., Salomon,W.E. and Zamore,P.D. (2012) Argonaute divides its RNA guide into domains with distinct functions and RNA-binding properties. *Cell*, **151**, 1055–1067.
41. Jung,S.R., Kim,E., Hwang,W., Shin,S., Song,J.J. and Hohng,S. (2013) Dynamic anchoring of the 3′-end of the guide strand controls the target dissociation of Argonaute-guide complex. *J. Am. Chem. Soc.*, **135**, 16865–16871.